AIAA JOURNAL
Vol. 30, No. 6, June 1992

Effects of Gas Density on the Structure of Liquid Jets in Still Gases

L.-K. Tseng,* G. A. Ruff,† and G. M. Faeth‡
University of Michigan, Ann Arbor, Michigan 48109

A theoretical and experimental study of the near jet-exit region of nonevaporating round liquid jets in still gases is described, emphasizing effects of ambient gas density in the atomization breakup regime where liquid breakup begins right at the jet exit. Mean liquid volume fraction distributions were measured for 9.5-mm-diam water jets in still air at pressures of 1–8 atm. Mixing was strongly affected by the gas/liquid density ratio and the degree of flow development at the jet exit, with the largest gas/liquid density ratio and fully developed turbulent pipe flow yielding the fastest mixing rates. Flow properties were predicted using the locally homogeneous flow approximation, where relative velocities between the phases are assumed to be small in comparison to mean flow velocities. Predictions were in good agreement with measurements, including representation of effects of gas/liquid density ratio and flow development at the jet exit, but only at relatively high mixture fractions. In contrast, separated flow effects caused predictions to overestimate rates of flow development at low mixture fractions.

Nomenclature

d = jet-exit diameter
f = mixture fraction
k = turbulence kinetic energy
L = injector passage length
Oh = Ohnesorge number, $\mu_f/(\rho_f d\sigma)^{1/2}$
p = pressure
r = radial distance
Re_f = jet Reynolds number, $\rho_f d u_o/\mu_f$
u = streamwise velocity
v = radial velocity
w = tangential velocity
We_{id} = Weber number based on phase i and the jet diameter, $\rho_i d u_o^2/\sigma$
x = streamwise distance
α = volume fraction
ε = rate of dissipation of turbulence kinetic energy
μ = molecular viscosity
ρ = density
σ = surface tension
ϕ = generic property

Subscripts

c = centerline value
f = liquid-phase property
g = gas-phase property
o = jet-exit conditions
∞ = ambient conditions

Superscripts

$(\bar{\ }),(\bar{\ })'$ = time-averaged mean and rms fluctuating quantities
$(\tilde{\ }),(\tilde{\ })''$ = Favre-averaged mean and rms fluctuating quantities

Received Jan. 26, 1991; revision received Aug. 14, 1991; accepted for publication Aug. 19, 1991.

*Graduate Assistant, Department of Aerospace Engineering.
†Graduate Assistant, Department of Aerospace Engineering; currently Assistant Professor, Department of Mechanical Engineering, Drexel University, Philadelphia, PA.
‡Professor, Department of Aerospace Engineering. Fellow AIAA.

Introduction

An experimental and theoretical investigation of the near jet-exit region of nonevaporating round liquid jets in still gases is described. This flow is of interest for a variety of atomization and gas/liquid mixing processes; it also merits study as the multiphase counterpart of the single-phase turbulent jet. The objective of the research was to extend earlier studies of round water jets in still room air,[1–3] to consider effects of ambient gas density on the structure and mixing properties of the flow. Measurements of liquid volume fraction distributions were completed for water jets in still air at various ambient pressures. Tests were limited to atomization breakup, where liquid breakup into drops and the development of a multiphase mixing layer begins right at the jet exit, because this regime is most important for practical applications.[4,5] Jet-exit conditions included both fully developed turbulent pipe flow and low-turbulence intensity slug flow due to the known importance of the degree of flow development at the jet exit on flow properties.[1–3,6] The measurements were used to evaluate predictions of effects of gas/liquid density ratio on flow properties, found from an earlier model based on the locally homogeneous flow (LHF) approximation where relative velocities between the phases are assumed to be small in comparison to mean flow velocities.[1]

Only the main features of past work are considered, because reviews treating multiphase jets and dense sprays have appeared recently.[7,8] Past measurements have established the main features of the near injector region of liquid jets in still gases within the atomization breakup regime. The flow consists of a liquid core, much like the potential core of a single-phase jet, surrounded by a dispersed drop/gas mixing layer. Conductivity probes have been used to study the length of the liquid core at various ambient gas densities.[6,9,10] The liquid core tends to become shorter at high ambient gas densities due to increased entrainment rates. Nevertheless, the liquid core and its multiphase mixing layer are prominent features of the flow for typical gas/liquid density ratios, extending 200–400 jet-exit diameters for liquid jets in still gases at atmospheric pressure.[9]

Recent measurements of Ruff et al.[1–3] have yielded some information about the structure of the near jet-exit region of liquid jets in still gases. These experiments involved large (9.5- and 19.1-mm initial diameters) water jets injected in still air at atmospheric pressure. Measurements included liquid volume fraction distributions using gamma-ray absorption, drop

sizes and velocities in the mixing layer using double-pulse holography, and air entrainment rates using laser velocimetry. The measurements of mean liquid volume fraction distributions showed that the rate of development of the flow was affected by both the breakup regime and the degree of flow-development at the jet exit: atomization breakup and fully developed turbulent pipe flow at the jet exit yielded the fastest mixing rates. Predictions based on the LHF approximation were effective for atomization breakup when mean liquid volume fractions were greater than 0.2; however, they progressively failed as the flow became dilute and as jet-exit conditions approached the wind-induced breakup regime. Difficulties with the LHF approach were identified by drop size and velocity measurements in the mixing layer, which showed significant effects of separated flow in regions where liquid volume fractions were low. Thus, the success of the LHF approximation at large liquid volume fractions was attributed to the small proportion of the momentum associated with the gas phase at these conditions due to the small gas/liquid density ratio of the flow. Similarly, entrainment rates are governed mainly by processes within the dilute portions of the mixing layer; therefore, LHF predictions generally overestimated entrainment rates due to separated-flow phenomena in the mixing layer. However, the findings suggested improved performance of LHF methods at large We_f, with this limit approached more rapidly at large gas/liquid density ratios.

The objective of the present investigation was to explore effects of gas/liquid density ratio on the mixing properties of liquid jets in still gases and the adequacy of predictions of flow properties based on the LHF approximation. Experiments involved measurements of liquid volume fraction distributions within large-scale (9.5-mm initial jet diameter) water jets in still air at ambient pressures of 1–8 atm. The measurements were compared with predictions based on the earlier LHF approach,[1,2] to determine whether this methodology could treat effects of varying gas/liquid density ratios.

The paper begins with brief descriptions of experimental methods and the LHF computations. Results are then described, considering liquid volume and mass fraction distributions in turn.

Experimental Methods

Apparatus

Experimental methods were similar to Ruff et al.,[1] except that the flow was contained within a large pressure vessel so that the pressure of the ambient air could be changed. A sketch of the apparatus appears in Fig. 1. The arrangement involves a steady water jet injected vertically downward in still air within a large windowed pressure vessel (1.5-m diameter × 4.5-m long with two pairs of opposite windows having maximum opening diameters of 250 mm). Access to the interior of the pressure vessel was provided by a manhole at the top of the vessel. A second port at the top provided entry points to supply water to the jet and electrical cables needed to control the jet traversing system.

City water was fed to the injector using a centrifugal pump. The water was collected in the bottom of the tank with the liquid level maintained by outflow to a drain. A grate located above the liquid level reduced splash back into the test area. The rate of water flow was adjusted using a bypass system and was measured using a turbine flow meter that was calibrated by collecting water for timed intervals.

The water injectors had exit diameters of 9.5 mm and were the same as those used by Ruff et al.:[1] one yielding slug flow with low turbulence intensities, the other yielding fully developed turbulent pipe flow. The slug flow injector consisted of a honeycomb flow straightener (1.6-mm cells, 25-mm long) and two screens to calm the flow (16 × 16 square mesh, 0.18-mm-diam wire) followed by a 13.6:1 area contraction to the jet exit. The contraction was designed following Smith and Wang[11] to yield uniform velocities at the jet exit. The fully developed flow injector had the same flow straightener and contraction area ratio, but the contraction was followed by a constant area passage 41 jet-exit diameters long.

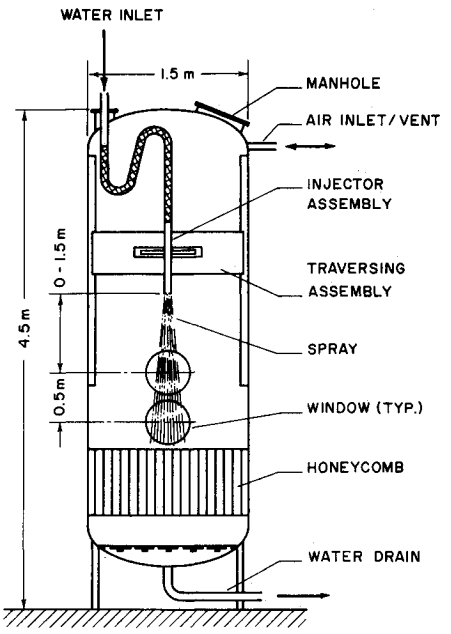

Fig. 1 Sketch of the variable gas density apparatus.

Instrumentation was mounted rigidly so that flow structure was measured by traversing the jet. Horizontal traverses were carried out using a stepping motor-driven linear positioner with a positioning accuracy of 5 μm. Vertical traverses involved moving the injector assembly along linear bearings with a manual positioner having a positioning accuracy of 0.5 mm.

Gamma-Ray Absorption Measurements

Distributions of mean liquid volume fractions were measured using gamma-ray absorption similar to Ruff et al.[1] An iodine-125 isotope source (5 mCi, emitting primarily at 27.20, 27.47 and 31.00 keV) provided a soft gamma-ray source with good absorption levels. The source was placed in a lead casket with an outlet aperture of 1.6-mm diameter and 13-mm long. Gamma rays passing through the flow were detected and counted with a Bicron X-ray probe (Model 1 × M.040/1.54) and a EG&G Ortec single-channel analyzer and counter/timer (models 556, 590A, and 974). A lead aperture (1.5-mm diameter and 12-mm long) was placed in front of the detector to define the path observed through the flow. The energy window of the detector was set at 22–32 keV to minimize spurious counts due to background radiation and Compton scattering. The source and detector were placed in recessed mounts within opposing windows of the apparatus (not shown in Fig. 1) so that they were separated by a distance of 500 mm with the radiation path crossing horizontally through the chamber axis.

Absorption measurements (based on 20,000–25,000 counts) were made for 30–60 parallel paths through the flow and deconvoluted in the same manner as Santoro et al.[12] and Ruff et al.[1] The narrow absorption path minimized potential errors due to the orientation of liquid elements to less than 5%.[13] Experimental uncertainties were largely due to finite sampling times and background from the small drops dispersed within the pressure vessel. They are estimated (95% confidence) to be less than 30% for $\bar{\alpha}_f > 0.01$.

Test Conditions

Test conditions are summarized in Table 1. Operating conditions were selected to yield the same mean jet exit velocity for fully developed and slug flow at pressures of 1, 2, 4, and

Table 1 Summary of test conditions[1]

Jet-exit diameter (mm)	9.5
Ambient pressure (atm)	1, 2, 4, and 8
Jet flow rate (kg/s)	3.47
Injector pressure drop (kPa):	
Fully developed flow	2270
Slug flow	2110
Average jet exit velocity (m/s)	49.1
Re_f	462,000
We_{fd}	312,000
We_{gd}	380, 760, 1520, 3040
Oh	0.00121

[a]Pressure-atomized water jet injected vertically downward in still air at various pressures and 298 ± 2K; in atomization breakup regime for both slug flow and fully developed turbulent pipe flow (L/d = 41) jet-exit conditions.

8 atm within the atomization breakup regime. Due to the limitations of the pump, this required a water flow rate roughly 13% lower than the atomization breakup condition used by Ruff et al.[1-3] for the 9.5-mm-diam injector. However, all test conditions are well into the atomization breakup regime defined by Ranz[4] and Miesse,[5] and exhibited initial liquid breakup right at the jet exit, which is characteristic of this breakup regime.

Flow properties at the jet exit were measured earlier using laser velocimetry.[1] For fully developed flow, mean streamwise velocity distributions were in good agreement with values in the literature for the same Reynolds number range.[14] However, rms streamwise and radial velocity fluctuations were more uniform across the central region, yielding streamwise and radial turbulence intensities of 7 and 4% near the axis, which are somewhat larger than literature values.[14] For slug flow, mean streamwise velocities were uniform over the central region of the flow and then declined near the wall (within 3–5% of the injector radius) due to boundary-layer growth in the nozzle passage. Streamwise and radial rms velocity fluctuations were roughly 1% of the mean streamwise velocity over the central region for slug flow.[1]

Theoretical Methods

Predictions of flow properties were limited to use of the LHF approximation similar to past work.[1,2,7] In addition to the LHF approximation, the major assumptions of the model are as follows: steady (in the mean) axisymmetric flow with no swirl, boundary-layer approximations apply, negligible kinetic energy and viscous dissipation of the mean flow, buoyancy only affects the mean flow, equal exchange coefficients of all species and phases, and negligible mass transport between the phases (no evaporation). These assumptions are either conditions of the experiments or are justified by past practice, except for the LHF approximation, which will be evaluated by the measurements. In particular, operation of well-atomized sprays within a closed container saturated the air with water vapor so that there was no potential for liquid evaporation.

Under these assumptions, the instantaneous mixture fraction (defined as the fraction of mass that originated from the injector) is either 0 (in the gas) or 1 (in the liquid). Then, time- and Favre-averages of any scalar property ϕ can be found in terms of the Favre-averaged mean mixture fraction, as follows:

$$\tilde{\phi} = \phi_\infty(1 - \tilde{f}) + \phi_o\tilde{f} \quad (1)$$

$$\overline{\phi} = (\phi_\infty\rho_0(1 - \tilde{f}) + \phi_o\rho_\infty\tilde{f})/(\rho_o(1 - \tilde{f}) + \rho_\infty\tilde{f}) \quad (2)$$

Given Eqs. (1) and (2), the flowfield can be found from a simplified version of the conserved-scalar formation of Lockwood and Naguib,[15] but using Favre averages following Bilger.[16] Governing equations are solved for conservation of mass, streamwise mean momentum, mean mixture fraction, turbulence kinetic energy, and the rate of dissipation of turbulence kinetic energy. The specific formulation, all empirical constants, and a discussion of calibration of the approach for a variety of constant and variable density single-phase jets, appears elsewhere.[7]

The specification of initial and boundary conditions, and the details of the numerical computations, can be found in Ruff et al.[1,2] For fully developed flow, initial profiles of $\tilde{u}$, k, and ε were taken from Schlichting[14] and Hinze[17] because they are good approximations of present measured jet-exit conditions and are readily available to others.[1] For slug flow, properties were assumed to be uniform except for bounding estimates of properties in the boundary layer along the wall for L/d = 0 and 5, with the latter conditions found assuming clean entry and no *vena contracta* along the nozzle passage from Schlichting.[14]

Results and Discussion

Mean Liquid Volume Fractions

Experimental Sensitivity

The mean liquid volume fraction distributions provide a quantitative indication of effects of gas/liquid density ratio and jet-exit conditions on flow properties. However, it is important to recognize the relationship between liquid volume fractions and mixing levels when interpreting these results. The present flows have large liquid/gas density ratios, which implies that liquid volume fractions vary rapidly with mixture fraction. This can be seen from the state relationship for liquid volume fraction:

$$\alpha_f = f/(f + (\rho_f/\rho_g)(1 - f)) \quad (3)$$

Using Eq. (2), an analagous expression can be obtained for time-averaged mixture fraction $\overline{\alpha}_f$, as a function of Favre-averaged mixture fraction $\tilde{f}$ as follows:

$$\overline{\alpha}_f = \tilde{f}/(\tilde{f} + (\rho_f/\rho_g)(1 - \tilde{f})) \quad (4)$$

Table 2 is a summary of f for α_f = 0.1 and 0.01 (or equivalently $\tilde{f}$ for the two values of $\overline{\alpha}_f$) over the present ambient pressure range. It is evident from the table that low levels of mixing cause large reductions in liquid volume fractions, even at the highest ambient pressures of the present test range. Thus, $\overline{\alpha}_f$ is an unusually sensitive indicator of mixing levels near the jet exit.

Axial Distributions

Measured and predicted time-averaged mean liquid volume fractions along the jet centerline are illustrated in Figs. 2 and 3 for fully developed and slug flow-jet exit conditions, respectively. Results are plotted as a function of distance from the injector, normalized by the injector diameter, with ambient pressure as a parameter. Predictions for slug flow jet-exit conditions are shown for L/d = 0 and 5, which bounds the potential degrees of flow development within the nozzle passage, as noted earlier. Measurements of Ruff et al.[1] at 1 atm for atomization breakup also are shown on the plots for both slug and fully developed flow; they agree very well with present results, although jet-exit velocities are slightly different. This is expected based upon the LHF predictions, which exhibit little variation of liquid volume fraction distributions with jet-exit velocity for the high Reynolds numbers of present flows.[1]

For fully developed flow, Fig. 2, the region near the jet exit (x/d < 3–8) exhibits mean liquid volume fractions near unity. Just beyond this region, however, mean liquid volume fractions decrease rapidly. The initial reduction of $\overline{\alpha}_{fc}$ occurs at progressively smaller values of x/d as the pressure increases, with values of $\overline{\alpha}_{fc}$ at a given value of x/d generally being lower

Table 2 f vs α_f for air/water mixtures[a]

	Pressure, atm			
α_f	1	2	4	8
0.10	0.990	0.979	0.960	0.923
0.01	0.897	0.813	0.684	0.520

[a]Air/water mixtures at 300 K and various pressures.

at higher pressures as well. These trends indicate faster mixing rates at higher ambient gas densities, analogous to effects of flow density ratio for single-phase turbulent jets.[18] There is good agreement between measurements and predictions, indicating that the LHF approach correctly treats effects of the density ratio of the flow on mixing properties. However, conditions illustrated in Fig. 2 represent relatively low levels of mixing; for example, results in Table 2 suggest that Favre-averaged mixture fractions are generally greater than 0.85. For such low levels of mixing, predictions based on the LHF approximation have been reasonably good in the past,[1] because separated flow effects due to relative velocity differences between the gas and liquid are not very significant when the mass of the flow is predominantly liquid. Based on past evaluations of the methodology,[7] performance of the LHF approach is likely to be poorer as the dilute dispersed flow regime (where $f << 1$) is approached; behavior in this regime is considered later. Finally, although the variation of $\bar{\alpha}_{fc}$ suggests a relatively short liquid core, this is not the case when viewed in terms of mixture fraction. Favre-averaged mixture fractions are greater than 0.85 for all the results illustrated in Fig. 2, so that even low levels of flapping of the liquid core can explain the reductions of $\bar{\alpha}_{fc}$.

The slug flow results illustrated in Fig. 3 exhibit slower rates of mixing than the fully developed flows. First, $\bar{\alpha}_{fc}$ remains at unity until x/d is in the range 20–50. Similar to the results for fully developed flow, however, the value of x/d where $\bar{\alpha}_{fc}$ first begins to decrease from unity progressively decreases as the pressure increases, implying faster rates of mixing at higher ambient densities. The strong effect of the degree of flow development at the jet exit (cf. Figs. 2 and 3) is similar to earlier observations at atmospheric pressure.[1] This occurs because the liquid density is large in comparison to the gas; therefore, the fully developed flow carries significant levels of turbulence energy into the mixing layer, which enhances mixing rates. Predictions of properties for slug flow conditions are very sensitive to the degree of flow development at the jet exit. Thus, there are significant differences between predictions for pure slug flow ($L/d = 0$) and allowance for boundary-layer growth within the injector passage ($L/d = 5$). These conditions bound the range of possibilities for present tests, and it is encouraging that the two predictions tend to bound the measurements except at $x/d = 100$ and pressures of 4 and 8 atm. The discrepancies at $x/d = 100$ occur in a region where the streamwise variation of flow properties is rapid, and tends toward dilute conditions. Thus, because both predictions tend to overestimate the rate of development of the flow, separated flow effects are probably responsible for the difficulty.

Radial Distribution (Fully Developed Flow)

Predicted and measured radial profiles of mean liquid volume fractions for fully developed flow are illustrated in Figs. 4 and 5 for ambient pressures of 1 and 8 atm (results at 2 and 4 atm are similar). These results involve $\bar{\alpha}_f/\bar{\alpha}_{fc}$ plotted as a function of radial distance normalized by the injector radius, so that the actual width of the flow can be seen. Results are shown for various $x/d \leq 100$ because larger distances risked disturbances of the flow from the chamber walls. The measurements of Ruff et al.[1] at 1 atm are illustrated in Fig. 4 along with the present results. The two sets of experiments

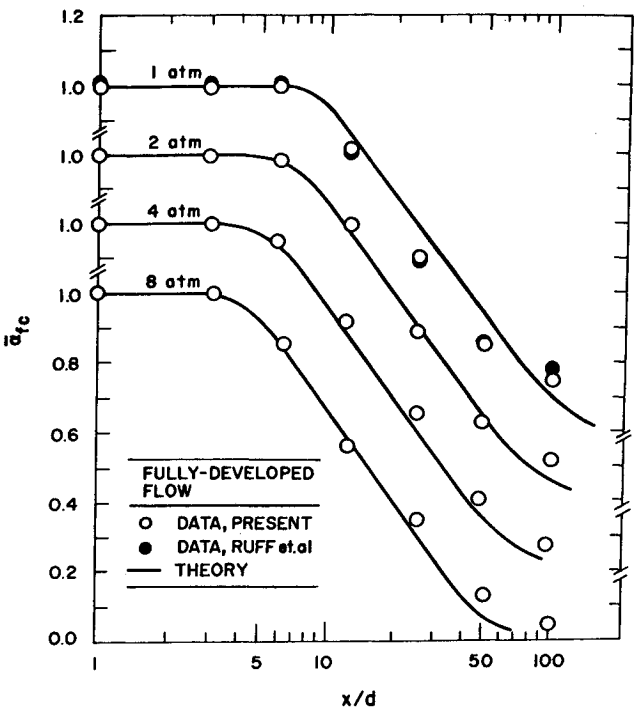

Fig. 2 Time-averaged liquid volume fractions along the axis at various ambient pressures for fully developed flow.

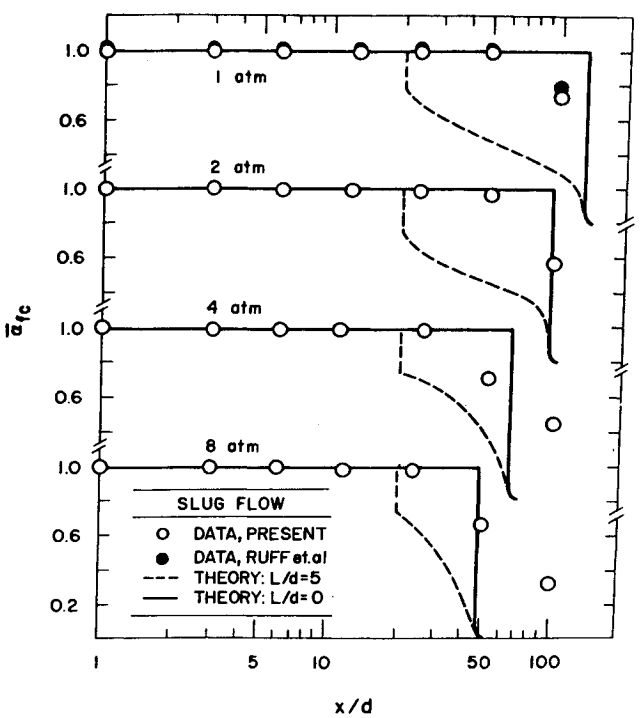

Fig. 3 Time-averaged liquid volume fractions along the axis at various pressures for slug flow.

agree within experimental uncertainties except at $x/d = 100$ where the confinement of the present jets may be responsible for somewhat reduced flow widths. As discussed earlier, predictions are essentially the same for the Reynolds number differences of the two tests. The measurements in Figs. 4 and 5 show a progressive increase of flow width with increasing distance from the jet exit, with flow widths increasing at a faster rate at the higher pressure. Apparent flow radii based on $\bar{\alpha}_f/\bar{\alpha}_{fc}$, however, are much smaller than for single-phase

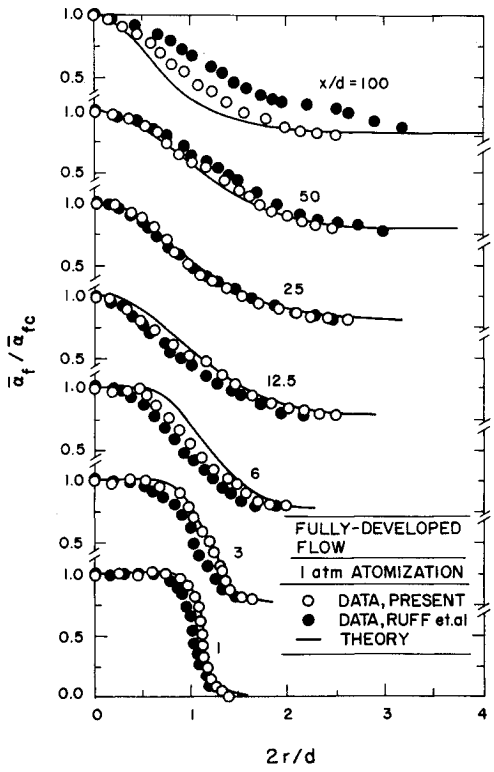

Fig. 4 Radial profiles of mean liquid volume fractions for fully developed flow at 1 atm.

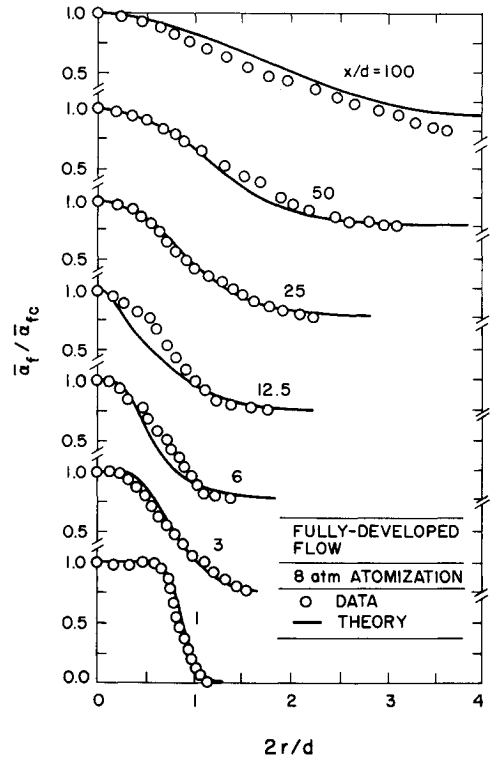

Fig. 5 Radial profiles of mean liquid volume fractions for fully developed flow at 2 atm.

jets because of the sensitivity of $\bar{\alpha}$ to the extent of mixing, discussed earlier. Notably, flow widths based on mean void fraction distributions for gas jets in liquids are unusually large for similar reasons.[19] For both turbulent liquid jets in gases and gas jets in liquids, however, predictions using the LHF approach indicate relatively normal flow widths far from the jet exit, in terms of $\bar{f}$: this is discussed more fully later.

The comparison between predicted and measured liquid volume fraction distributions in Figs. 4 and 5 is generally quite good, consistent with the good predictions of properties along the axis for fully developed flow observed in Fig. 2. The main exception is the farthest downstream position, $x/d = 100$, at 1 atm, where measurements exhibit a wider flow than predictions. Ruff et al.[1,2] show that this difficulty is largely due to effects of separated flow as the multiphase flow becomes more dilute. Predictions at $x/d = 100$ are improved at 8 atm, which is expected, because the larger gas density should yield smaller drops after secondary breakup, tending to reduce errors due to effects of separated flow.[2,3]

Radial Distributions (Slug Flow)

Predicted and measured radial profiles of mean liquid volume fractions for slug flow are illustrated in Figs. 6 and 7 for ambient pressures of 1 and 8 atm (results at 2 and 4 atm are similar). Measurements of Ruff et al.[1] at 1 atm for slug flow are illustrated in Fig. 6 along with the present measurements. In this case, both sets of measurements agree everywhere within experimental uncertainties, in accord with expectations from the predictions. Better agreement between the two sets of measurements for slug flow than fully developed flow at $x/d = 100$ is reasonable because the slug flow is narrower, which reduces effects of confinement for present measurements. Predictions for $L/d = 0$ and 5 are shown, similar to Fig. 3. Results illustrated in Figs. 6 and 7 exhibit a relatively sharp transition between the liquid core of the flow and the region where $\bar{\alpha}_f$ decreases, at least for $x/d \leq 50$. Additionally, the extent of radial spread of the slug flows is less than the fully developed flows. Both these observations are consistent with slower mixing rates for slug flow than fully developed flow. As before, however, flow widths at a particular x/d are significantly larger at 8 atm than 1 atm, suggesting faster mixing rates at higher pressures.

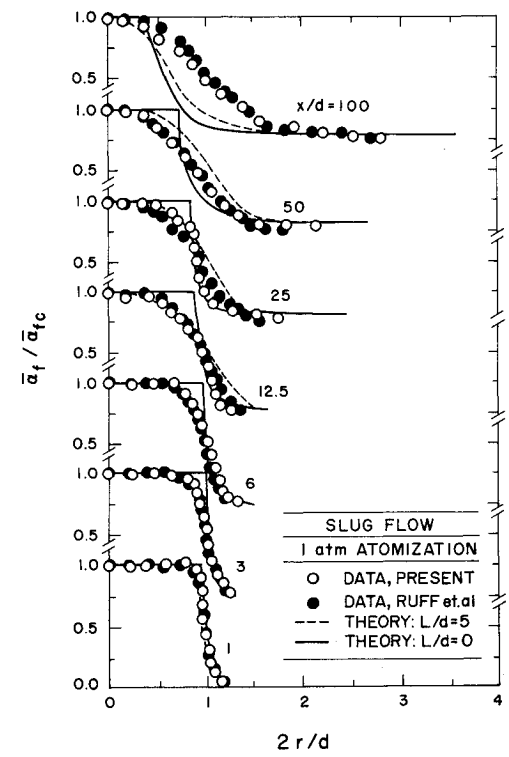

Fig. 6 Radial profiles of mean liquid volume fractions for slug flow at 1 atm.

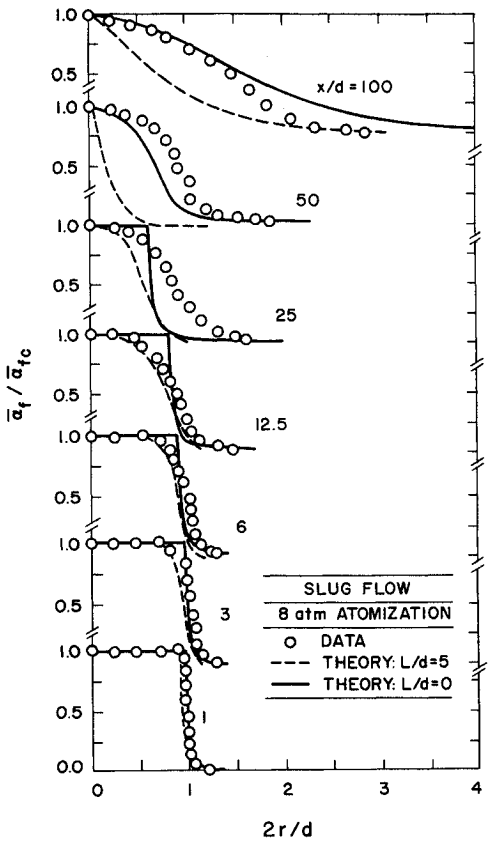

Fig. 7 Radial profiles of mean liquid volume fractions for slug flow at 2 atm.

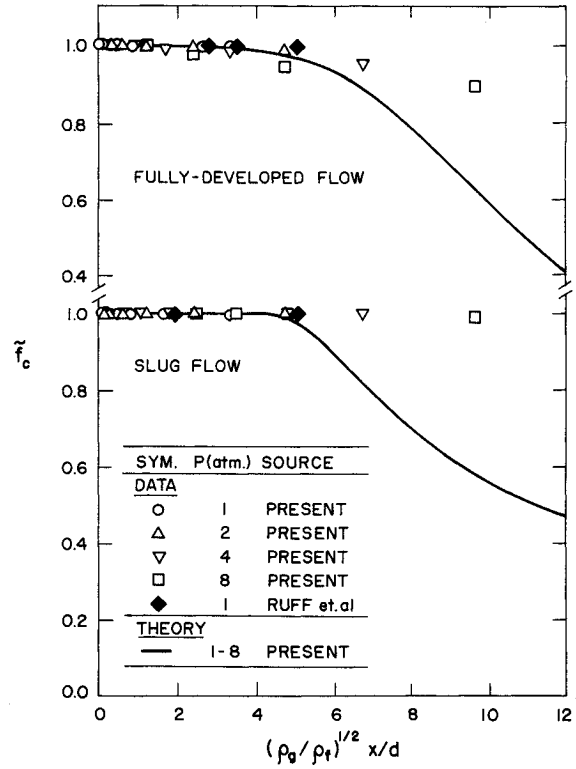

Fig. 8 Favre-averaged mixture fractions along the axis for fully developed and slug flow.

Predictions of slug flow properties in Figs. 6 and 7 are reasonably good for $x/d \leq 25$, within the bounds of the limiting estimates of the degree of flow development at the jet exit. Farther from the injector, however, predictions are less satisfactory. In particular, errors are large in the region where $\bar{\alpha}_{fc}$ first begins to decrease from unity (see Fig. 3). This behavior is caused by poor estimates of $\bar{\alpha}_{fc}$, due to uncertainties in the initial degree of flow development, because $\bar{\alpha}_{fc}$ is used to normalize both predictions and measurements in Figs. 6 and 7. Beyond this region, predictions are in better agreement with measurements but this is largely fortuitous because $\bar{\alpha}_{fc}$ is still not predicted very well by either limiting condition (see Fig. 3). These difficulties are probably due to the effects of separated flow in the rapidly developing region near the tip of the liquid core for slug flow, as discussed earlier.

Sensitivity Study

The sensitivity of present computations was examined similar to past work.[1,2] Predictions were very sensitive to initial mean velocity distributions, as can be seen from the results illustrated in Figs. 3, 6, and 7 for slug flow at the limits L/d = 0 and 5. Predictions were also sensitive to initial values of k and ε, with 10% changes in these properties causing 5–10% changes in $\bar{\alpha}_{fc}$ for x/d in the range 20–60. However, these properties were reasonably well known for the fully developed flows, whereas effects of low-turbulence levels in the case of the slug flow were not very significant. Thus, the uncertainties of the predictions were largely governed by difficulties in specifying the mean velocity distribution for slug flows, and the less quantifiable limitations of κ-ε turbulence models using the LHF approximation for multiphase boundary-layer flows.

Favre-averaged Mixture Fractions

Axial Distributions

Computations indicated that distributions of Favre-averaged mixture fractions were much less influenced by variations of ambient gas density than time-averaged liquid volume fractions; therefore, both present measurements and those of Ruff et al.[1-3] were examined in terms of this fundamental mixing property. This was done by computing $\tilde{f}$ from the measured values of $\bar{\alpha}$ using Eq. (4).

It is well known that properties along the axis of single-phase variable-density jets should scale in terms of a density-weighted streamwise distance, which becomes $(\rho_g/\rho_f)^{1/2}\, x/d$ for present measurements.[18] Chehroudi et al.[9] also find similar scaling for their correlation of the length of the liquid core. Thus, predicted and measured $\tilde{f}_c$ are plotted in terms of this variable for both fully developed and slug flows in Fig. 8. Measurements are identified by ambient pressure and source. When plotted in the manner of Fig. 8, predicted effects of ambient pressure, jet-exit Reynolds number, and L/d (for slug flow) were small; therefore, only single predicted lines are shown for fully developed and slug flow.

In contrast to $\bar{\alpha}_{fc}$, the sensitivity of present experiments to $\tilde{f}_c$ is relatively low due to the large density ratios of the flows. Thus, measured values of $\tilde{f}_c$ are generally greater than 0.85 as noted in connection with the plots of $\bar{\alpha}_{fc}$ (Figs. 2 and 3). Over this narrow range of $\tilde{f}_c$, however, the measurements at various ambient pressures correlated reasonably well in terms of density-weighted streamwise distance.

Predicted and measured $\tilde{f}_c$ shown in Fig. 8 are in reasonably good agreement for $(\rho_g/\rho_f)^{1/2}\, x/d < 5$. However, this observation is much less definitive than comparisons between predicted and measured values of $\bar{\alpha}_{fc}$ due to the reduced sensitivity of $\tilde{f}_c$. Similarly, the striking effect of jet-exit turbulence on the variation of $\bar{\alpha}_{fc}$ is much less evident for $\tilde{f}_c$. The measurements, however, yield larger values of $\tilde{f}_c$ than predicted at density-weighted distances greater than five, particularly for slug flow where predicted properties vary most rapidly in the streamwise direction. This implies slower rates of mixing along the axis than LHF predictions, suggesting significant effects of separated flow in the region just downstream of the end of the liquid core. This is plausible, because breakup of the end of the liquid core, the same as primary breakup along its

surface, should yield larger drops having significant relative velocities. Thus, the predicted universal behavior of $\tilde{f}_c$ was not approached for present test conditions as the flow become more dilute for density-weighted streamwise distances greater than five. This is much more evident from the plots of $\tilde{f}_c$ in Fig. 8 than those for $\bar{\alpha}_{fc}$ in Figs. 2 and 3 due to effects of large density ratio on sensitivity to these properties.

Radial Distributions

Due to the length of the liquid core, present flows are transitional between a mixing layer and a jet when viewed in the radial direction. Thus, radial profiles of $\tilde{f}$ were limited to mixing layer conditions ($\tilde{f}_c \approx 1$) to avoid the complications of this transition. Within the mixing layer, predictions showed that $\tilde{f}/\tilde{f}_c$ was relatively independent of the density ratio when plotted in terms of $(r - r_{\tilde{f}=0.5})/x$ so that measurements will be considered in terms of these variables. In order to extend the range of $\tilde{f}$ that could be examined, the present gamma-ray absorption measurements were supplemented by holography measurements in the multiphase mixing layer from Ruff et al.[2]

Predicted and measured radial profiles of $\tilde{f}/\tilde{f}_c$ are plotted in Fig. 9 for both fully developed and slug flows. As mentioned earlier, predictions exhibit small changes with density ratio and position for present test conditions. The present gamma-ray absorption measurements are in reasonably good agreement with predictions when plotted in the manner of Fig. 9, however, they are limited to $\tilde{f}/\tilde{f}_c > 0.85$.

The agreement between predictions and the holography measurements illustrated in Fig. 9 is much less satisfactory. The holography measurements were obtained in the dispersed flow region where the liquid is present as irregular liquid elements and drops, which is typical of dilute dispersed flows. Thus, poorer performance of the LHF approximation is expected, based on observations in other dilute dispersed flows.[8]

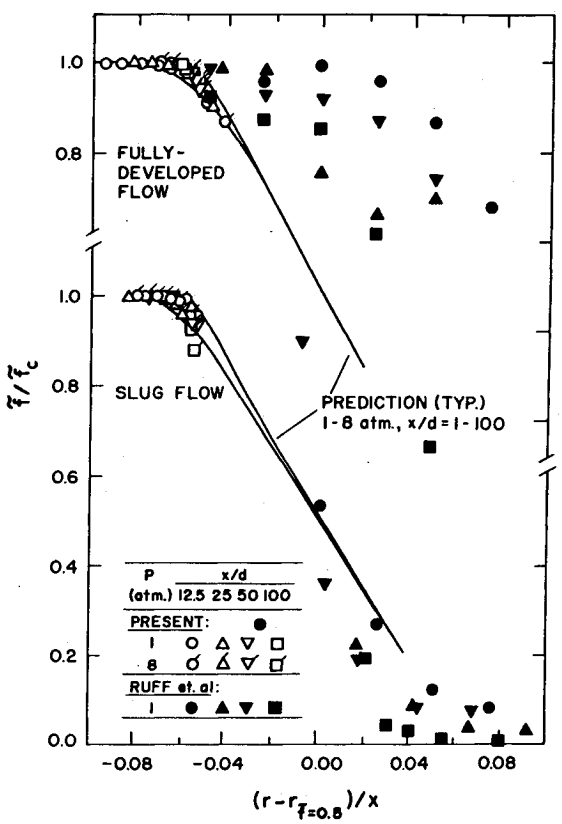

Fig. 9 Radial profiles of Favre-averaged mixture fractions in the multiphase mixing layer for fully developed and slug flow.

Nevertheless, the holographic measurements for slug flow conditions do approach predictions, with predicted overestimation of the mixing rates near the outer edge of the flow being attributable to separated flow effects. Discrepancies between predictions and measurements, however, are much larger for fully developed flow. Nevertheless, this behavior is reasonable because drop sizes after primary breakup were much larger for the fully developed flow than the slug flow (SMD of 1330 μm as opposed to 174 μm), which implies greater effects of separated flow.[3] Thus, improved atomization conditions might yield the universal results suggested by the predictions; however, additional measurements are needed to evaluate this possibility.

A final matter to be considered in connection with Fig. 9 is why the holography measurements show faster mixing than predicted for fully developed flow but slower mixing than predicted for slug flow. This behavior is caused by interactions between primary breakup and separated-flow phenomena.[3] Primary breakup of a turbulent liquid generates large liquid elements with radial velocities comparable to radial velocity fluctuations in the liquid. Thus, these large liquid elements are projected across the dispersed flow before they break up or relax to local flow velocities, which enhances mixing. In contrast, primary breakup of nonturbulent liquids yields small radial velocities, while large drops have poor response to turbulent dispersion due to their inertia, which retards mixing.

Conclusions

The structure and mixing properties of nonevaporating liquid jets in still gases were studied for various ambient gas densities at atomization breakup conditions, emphasizing the region near the jet exit. The major conclusions of the study are as follows:

1) Increasing gas/liquid density ratios reduces the length of the liquid core and increases the flow width, implying increased rates of mixing analogous to effects of density ratio for single-phase turbulent jets.

2) Turbulence levels and the degree of flow development at the jet exit have a strong effect on mixing rates, with turbulent flows mixing much faster than nonturbulent slug flows.

3) Use of the locally homogeneous flow approximation, in conjunction with a Favre-averaged turbulence model, yielded good estimates of effects of gas/liquid density ratio and initial liquid vorticity on time-averaged liquid volume fraction distributions and Favre-averaged mixture fraction distributions in the region near the liquid core where $\tilde{f} > 0.85$. The main reason for this is that separated flow effects, like small velocities of the gas and small drops, are not very important for these low degrees of mixing. Nevertheless, it is helpful that predictions provide reasonable estimates of the initial stages of mixing.

4) Distributions of $\tilde{f}$ were relatively independent of the density ratio of the flow in terms of $(\rho_g/\rho_f)^{1/2}\, x/d$ along the axis and $(r - r_{\tilde{f}=0.5})/x$ across the mixing layer for $\tilde{f} > 0.85$; therefore, many of the unusual mixing properties of these flows in terms of $\bar{\alpha}_f$ are due to the strong nonlinearities of the state relationship between α_f and f rather than unusual behavior of the fundamental mixing variable $\tilde{f}$ itself. Predictions suggest that this scaling of $\tilde{f}$ should extend to the full range of f if effects of separated flow are small; however, this regime was not reached during the present experiments.

5) For $\tilde{f} < 0.85$, significant effects of separated flow were observed, causing poor performance of predictions using the locally homogeneous flow approximation and effects of the density ratio on the scaling of distributions of $\tilde{f}$. This agrees with other determinations of important effects of separated flow in dilute dispersed flows, however, quantitative estimates of conditions where separated-flow must be considered require more information on primary breakup properties than is currently available.

Present conclusions are based on large-scale sprays (9.5-mm injector diameter) that have much lower rates of deceleration than practical injectors, and regions of the flow having relatively high mixture fractions (generally greater than 0.9 along the axis) where the momentum of the gas does not have a strong influence on flow dynamics. These factors favor use of the locally homogeneous flow approximation, so that present observations are not necessarily in conflict with earlier work showing significant separated-flow effects within dense sprays for smaller injector diameters and mixture fractions.[1-3,7] Additional information concerning liquid breakup properties in dense sprays clearly is needed in order to provide a rational means of evaluating separated-flow effects and the adequacy of the locally homogeneous flow approximation for particular conditions.

Acknowledgments

This research was supported by ONR Grant N00014-89-J-1199 with G. D. Roy serving as Scientific Officer. Initial development of the variable ambient density test chamber was sponsored by the Air Force Office of Scientific Research, under Grant No. AFOSR-85-0244, with J. N. Tishkoff serving as Program Manager. The U.S. Government is authorized to reproduce and distribute copies of this paper for governmental purposes notwithstanding any copyright notation thereon.

References

[1]Ruff, G. A., Sagar, A. D., and Faeth, G. M., "Structure and Mixing Properties of Pressure-Atomized Sprays," *AIAA Journal*, Vol. 27, No. 7, 1989, pp. 901–908.

[2]Ruff, G. A., Bernal, L. P., and Faeth, G. M., "Structure of the Near-Injector Region of Non-Evaporating Pressure-Atomized Sprays," *Journal of Propulsion and Power*, Vol. 7, No. 2, 1991, pp. 221–230.

[3]Ruff, G. A., Wu, P.-K., Bernal, L. P., and Faeth, G. M., "Continuous- and Dispersed-Phase Structure of Dense Nonevaporating Pressure-Atomized Sprays," *Journal of Propulsion and Power*, in press.

[4]Ranz, W. E., "Some Experiments on Orifice Sprays," *Canadian Journal of Chemical Engineering*, Vol. 36, No. 8, 1958, pp. 175–181.

[5]Miesse, C. C., "Correlation of Experimental Data on the Disintegration of Liquid Jets," *Industrial Engineering Chemistry* Vol. 47, No. 9, 1955, pp. 1690–1697.

[6]Phinney, R. E., "The Breakup of a Turbulent Jet in a Gaseous Atmosphere," *Journal of Fluid Mechanics*, Vol. 6, Oct. 1973, pp. 689–701.

[7]Faeth, G. M., "Mixing, Transport and Combustion in Sprays," *Progress in Energy and Combustion Science*, Vol. 13, No. 4, 1987, pp. 293–345.

[8]Faeth, G. M., "Structure and Atomization Properties of Dense Turbulent Sprays," *Twenty-Third Symposium (International) on Combustion*, The Combustion Institute, Pittsburgh, PA, 1990, pp. 1345–1352.

[9]Chehroudi, B., Onuma, Y., Chen, S.-H., and Bracco, F. V., "On the Intact Core of Full Cone Sprays," Society of Automotive Engineers Paper 850126, 1985.

[10]Hiroyasu, H., Shimizu, M., and Arai, M., "The Breakup of a High speed Jet in a High Pressure Gaseous Environment," Univ. of Wisconsin, Madison, ICLASS-82, 1982.

[11]Smith, R. H., and Wang, C.-T., "Contracting Cones Giving Uniform Throat Speeds," *Journal of Aeronautical Science*, Vol. 11, No. 10, 1944, pp. 356–360.

[12]Santoro, R. J., Semerjian, J. H., Emmerman, P. J., and Goulard, R., "Optical Tomography for Flow Field Diagnostics," *International Journal of Heat and Mass Transfer*, Vol. 24, No. 7, 1981, pp. 1139–1150.

[13]Gomi, H., and Hasegawa, K. I., "Measurements of the Liquid Phase Mass in Gas-Liquid Sprays by X-ray Attenuation," *International Journal of Multiphase Flow*, Vol. 10, No. 4, 1984, pp. 653–662.

[14]Schlichting, H., *Boundary Layer Theory*, 7th ed., McGraw-Hill, New York, 1979, p. 599.

[15]Lockwood, F. C., and Naguib, A. S., "The Prediction of Fluctuations in the Properties of Free, Round-Jet Turbulent Diffusion Flames," *Combustion and Flame*, Vol. 24, No. 1, 1975, pp. 109–124.

[16]Bilger, R. W., "Turbulent Jet Diffusion Flames," *Progress in Energy and Combustion Science*, Vol. 1, No. 1, 1976, pp. 87–109.

[17]Hinze, J. O., *Turbulence*, 2nd ed., McGraw-Hill, New York, 1975, p. 427 and pp. 724–734.

[18]Ricou, F. P., and Spalding, D. B., "Measurements of Entrainment by Axisymmetrical Turbulent Jets," *Journal of Fluid Mechanics*, Vol. 11, Jan. 1961, pp. 21–32.

[19]Loth, E., and Faeth, G. M., "Structure of Underexpanded Round Air Jets Submerged in Water. *International Journal of Multiphase Flow*, Vol. 15, No. 4, 1989, pp. 589–603.